2012

A Microwave Radiometer Roughness Correction Algorithm For Sea Surface Salinity Retrieval

Yazan Henry Hejazin
University of Central Florida

A MICROWAVE RADIOMETER ROUGHNESS CORRECTION ALGORITHM FOR SEA SURFACE SALINITY RETRIEVAL

by

YAZAN HENRY HEJAZIN

B.S. Princess Sumaya University for Technology, 2010

A thesis submitted in partial fulfillment of the requirements for the degree of Master of Science in Electrical Engineering in the Department of Electrical Engineering and Computer Science at the University of Central Florida

Orlando, Florida

Spring Term

2012

Major Professor: Linwood Jones

ABSTRACT

The Aquarius/SAC-D is an Earth Science remote sensing satellite mission to measure global Sea Surface Salinity (SSS) that is sponsored by the NASA and the Argentine Space Agency (CONAE). The prime remote sensor is the Aquarius (AQ) L-band radiometer/scatterometer, which measures the L-band emitted blackbody radiation (brightness temperature) from the ocean. The brightness temperature at L-band is proportional to the ocean salinity as well as a number of physical parameters including ocean surface wind speed. The salinity retrieval algorithm make corrections for all other parameters before retrieving salinity, and the greatest of these is the increased brightness temperature due to roughness caused by surface wind speed. This thesis presents an independent approach for the AQ roughness correction, which is derived using simultaneous measurements from the CONAE Microwave Radiometer (MWR).

When the wind blows over the ocean's surface, the brightness temperature is increased because of the ocean wave surface roughness. The MWR provides a semi-empirical approach by measuring the excess ocean emissivity at 36.5 GHz and then applying radiative transfer theory (improved ocean surface emissivity model) to translate this to the AQ 1.4 GHz frequency (L-band). The theoretical basis of the MWR algorithm is described and empirical results are presented that demonstrate the effectiveness in reducing the salinity measurement error due to surface roughness.

To my parents

ACKNOWLEDGMENTS

I want to thank my major advisor Dr. Linwood Jones for the time, effort and dedication he has exploited to make this work possible. He taught me how a hard work can be very fruitful and satisfying.

Also I would like to thank my committee members Dr. Wasfy Mikhael and Dr. Lei Wei for their interest and time. I am thankful to my team members at Central Florida Remote Sensing Laboratory (CFRSL), for their assistance and support, namely, Dr. Salim AlNimri, Dr. Suleiman AlSweiss, Dr Sayak Biswas and Spencer Farrar.

I would like to take the chance to thank Mr. Simon Yueh and Mr. Liang Hong, for helping me through this research and being a big support.

Finally I wish to acknowledge the financial support provided by the Aquarius SAC/D project funded by NASA/JPL.

TABLE OF CONTENTS

LIST OF FIGURES

LIST OF TABLES

CHAPTER ONE: INTRODUCTION

Sea surface salinity (SSS), defined as the concentration of dissolved salt in water, is an important geophysical parameter in the study of the Earth's climate change. Global salinity measurements from space can help geophysicists to unravel the ambiguity pertaining two major components of the earth's climate system: hydrological (water) cycle and ocean circulation. The measurement of salinity is a "tracer" can give an indicator of how the natural reciprocation of water between the ocean, atmosphere and sea ice influences the ocean circulation and therefore the climate [1].

Earth is the "Ocean Planet" therefore the ocean is the dominant player in the Earth's water cycle between ocean, atmosphere, and land. Salinity varies spatially and temporally, and SSS can be essential to understanding the ocean's eminent role in the Earth's water cycle, for which "approximately 86 percent of global evaporation and 78 percent of global precipitation occur over ocean". By measuring salinity changes caused by ice melting, precipitation (rain and snow) and rivers runoff, scientists can gather information of how the water transfers around the Earth between land, ocean and the atmosphere [2].

Salinity and temperature determine the ocean density (mass/unit-volume), and variations in water density cause the flow of ocean currents, which are a key factor of distributing the heat between the tropics and the poles [1]. Because of this vital role of salinity in ocean circulation, NASA has set a science goal to provide global satellite salinity measurements to oceanographers and climate scientists to improve computer models used for forecasting climate conditions and to understand the correlation between salinity changes and water cycle, ocean circulation and climate. Under the NASA Earth System Science Pathfinder Program, the Aquarius satellite mission will provide accurate salinity maps of the entire ocean every seven days. These weekly maps will track any changes in salinity from month to month, season to season and year to year [2].

1.1 Aquarius Mission Overview

Aquarius is an earth observations satellite science mission, with the objective to provide global, long-term salinity measurements that will improve scientists' understanding of ocean's water cycle and climate changes by monitoring changes in ocean's salinity and its effect on ocean currents.

The mission is a partnership between the United States (NASA) and the Argentina's space agency, Comisión Nacional de Actividades Espaciales (CONAE). The satellite was launched on June 10, 2011 from Vandenberg Air Force Base in California, and it fly's in a sun-synchronous polar orbit with an altitude of 657 kilometers and an inclination of (98°). The orbit has an exact repeat every 7 days, which is required for the prime instrument to completely cover the oceans. This meets the mission's requirements of generating salinity maps of the entire ocean once a week at a resolution of 150 kilometers [2]. An artist illustration of the Aquarius satellite is presented in Figure 1.

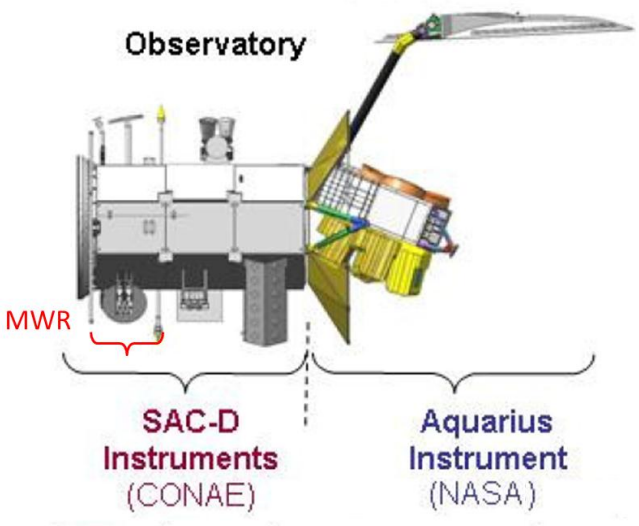

Figure 1 Aquarius/SAC-D Observatory

For the salinity measurements, the instruments are Aquarius (prime) and MicroWave Radiometer (MWR – secondary) that are shown in figure 1. Aquarius (AQ) is the name of the prime mission instrument, a passive/active (radiometer/scatterometer) L-band remote sensor developed by the NASA, Goddard Space

Flight Center (GSFC) and the Jet Propulsion Laboratory (JPL). MWR is a CONAE supplied instrument that supports AQ and is used to measure and detect rain, sea ice, and wind speed. These instruments are mounted on the Argentina-built spacecraft, Satélite de Aplicaciones Científicas SAC-D [3].

1.2 Problem Statement

The reason that makes measuring brightness temperature at 1.41 GHz a very challenging and laborious task, is that at this frequency, the signal is weak and can be easily interfered by noise (unwanted signals), and that imposes certain number of errors to the measurements. Table 1.1 illustrates the errors induced to salinity measurements due to instrumental and geophysical parameters. Based on that, the key factor that introduces the largest error is the surface roughness.

Table 1 Tb Error Budget

Error source	3 Beam RMS
Radiometer	0.15
Antenna	0.08
System pointing	0.05
Roughness	0.28
Solar	0.05
Galactic	0.05
Rain (Total liquid water)	0.02
Ionosphere	0.06
Atmosphere	0.05
SST	0.1
Antenna gain near land & ice	0.1
Model function	0.08

Precise corrections should be done to alleviate the effect of wind speed perturbation on the measured brightness temperatures used to retrieves salinity, and maintain a ±0.2 psu accuracy within the very small range of ocean's salinity (32-37 psu) to meet the AQ science goal [2]. Therefore, this thesis proposes improving AQ salinity retrievals by reducing the biases associated with Tb, by correcting for the main error source; oceanic winds (surface roughness).

1.3 Objectives Of This Research

A baseline approach in this thesis is to improve the AQ microwave radiometer salinity retrievals by correcting for the effect of geophysical parameters (wind speed) on measured brightness temperature.

The L-band (1.26 GHz) radar scatterometer is going to measure simultaneous ocean backscatter in the footprint, which will be used to calculate the roughness that caused the brightness temperature to increase. Separate algorithms for H polarization and V polarization are used to generate multiple linear regressions to relate the roughness with the excess brightness temperature, hence, find the effect of wind speed over the brightness temperature measurements and eliminate it.

This thesis provides calibration/validation of the ocean salinity measurements provided by AQ radiometer, and to introduce a correction algorithm of the effect of wind speed over the salinity retrieval, and validating this algorithm by doing comparisons between SSS and reading made by the situ buoy instruments. Those algorithms will remove any biases and dependence on wind speed and techniques to characterize these errors will be evaluated.

CHAPTER TWO: AQUARIUS INSTRUMENT

2.1 Aquarius Instrument Description

Aquarius/SAC-D satellite is a partnership mission between The United States (NASA) and Argentina (CONAE). It was launched on June, 10th 2011 from Vandenberg Air Force Base in California.

The observatory comprises Aquarius instrument developed by NASA (main instrument) and other instruments provided by CONAE and its partners. A complete list of instruments and their individual characteristics is shown in table 2.1 [3].

Aquarius is a microwave radiometer/scatterometer instrument operating at L-band. The radiometer is the passive part if AQ and is built to map the ocean salinity, and the scatterometer is the active part built to provide simultaneous surface roughness correction (major source error in salinity measurements).

Table 2 Aquarius SAC-D instruments

Instrument	Objective	Description	Resolution	Source
Aquarius	Sea surface salinity	• Integrated 1.41 GHz polarimetric radiometer • 1.26 GHz scatterometer • 390 km swath	3 Beams • 76 x 94 km • 84 x 120 km • 96 x 156 km	NASA
MWR **Microwave Radiometer**	Precipitation, wind speed, sea ice concentration, water vapor	• 23.8 GHz and 36.5 GHz • Dual polarized • 390 km swath	• 40 km	CONAE

Instrument	Objective	Description	Resolution	Source
NIRST **New Infrared Sensor Technology**	Hot spots (fires), sea surface temperature	• Bands: 3.8, 10.7, and 11.7 µm • Swath: 180km	• 350 m	CONAE
HSC **High Sensitivity Camera**	Urban lights, fires, aurora	• Bands: 450-900 µm • Swath: 700 km	• 200-300 m	CONAE
DCS **Data Collection System**	Environmental data collection	• Band: 401.55 MHz uplink	• 2 contacts/day with 200 platforms	CONAE
ROSA **Radio Occultation Sounder for Atmosphere**	Atmosphere temperature and humidity profiles	• GPS occultation	• Horizontal: 300 km • Vertical: 300 km	ASI (Italy)
Instrument	Objective	Description	Resolution	Source
CARMEN 1 **ICARE and SODAD**	ICARE: Effect of cosmic radiation on electronics SODAD: Effect of micro-particles and space debris	• ICARE: Three depleted Si and Si/Li detectors • SODAD: Four SMOS sensors	• ICARE: 256 channels • SODAD: 0.5 µ at 20 km/s sensitivity	CNES (France)

2.1.1 Radiometer

The radiometer part of the AQ comprises a 2.5 meters offset parabolic reflector and three feeds, transferring the collected brightness temperature to three separate Dicke radiometers through three waveguides [5].

The three feed horns image in pushbroom fashion, pointed roughly perpendicular to the spacecraft's flight direction, facing the night side of the orbit away from the sun – to avoid solar contamination – [3]. The inner and the outer beams point slightly forward, while the middle beams points slightly afterward [6]. Figure 2 illustrates the SAC-D and the AQ beams.

The three beams point at incidence angles 28.7^{o}, 37.8^{o} and 45.6^{o} for the inner, middle and outer beams respectively. And those beams create three instantaneous fields of view (IFOV's) at the intersection with the Earth's surface with a resolution of 79x94 km for inner beam, 84x120 km for middle beam and 96x156 km for outer beam [6].

The three beams together, map a swath of 390 km with spatial resolution of 150 km to allow a repetition of 7 days exactly, which is significant for salinity monthly averaging [7].

An additional polarimetric operation is included (third stoke measurement) to help correcting for the Faraday angle rotation [6]. Furthermore, a tight thermal control is embedded to achieve the stability required for the averaging [3].

The radiometer was designed to provide global salinity maps on monthly basis, with an accuracy of 0.2 psu.

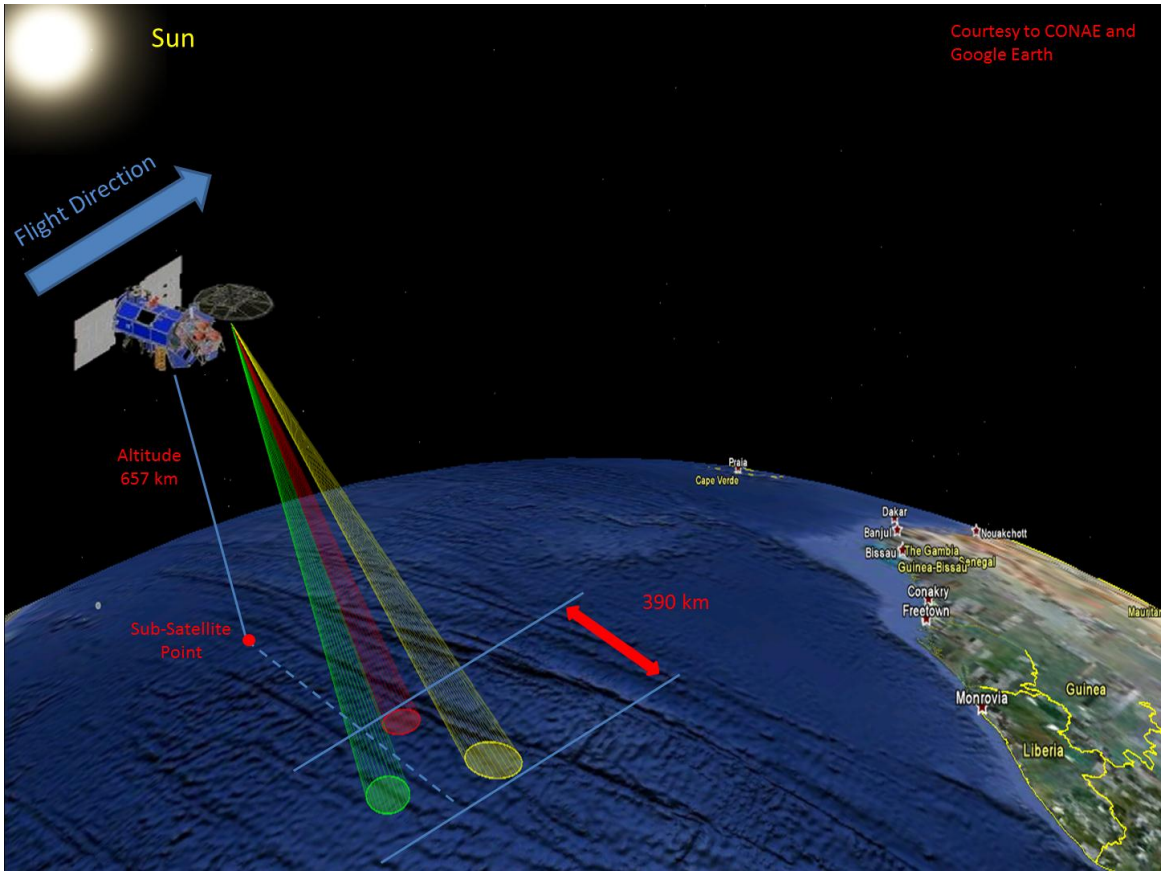

Figure 2 SAC-D with AQ Beams

2.1.2 Scatterometer

The AQ scatterometer is an active sensor (Radar) operating at L-band frequency (1.26 GHz). Its purpose is to estimate sea surface roughness that can perturb the radiometer signal by several degrees. Those estimations are potential corrections for the wind speed effect on measured brightness temperatures that will be later used to retrieve salinity [8], where the windy conditions correspond to stronger backscatter signal received by the scatterometer.

Although AQ has three separate radiometers, it has one scatterometer which circulates among the three feeds and both polarizations. Both radiometer and scatterometer will monitor the same pixel at the same instant of time. The scatterometer will create three IFOV's that share the same incidence angle and

boresight location with the radiometer IFOV's, and cover a swath of 370km (smaller than radiometer). Figure 3 shows the radiometer 3dB footprint (solid lines) and the scatterometer 3dB footprint (dashed lines) [7].

AQ scatterometter transmits a 1 ms (1 millisecond) pulse with a 100 Hz pulse repetition frequency (PRF), which results in 10 ms between the pulses [6].

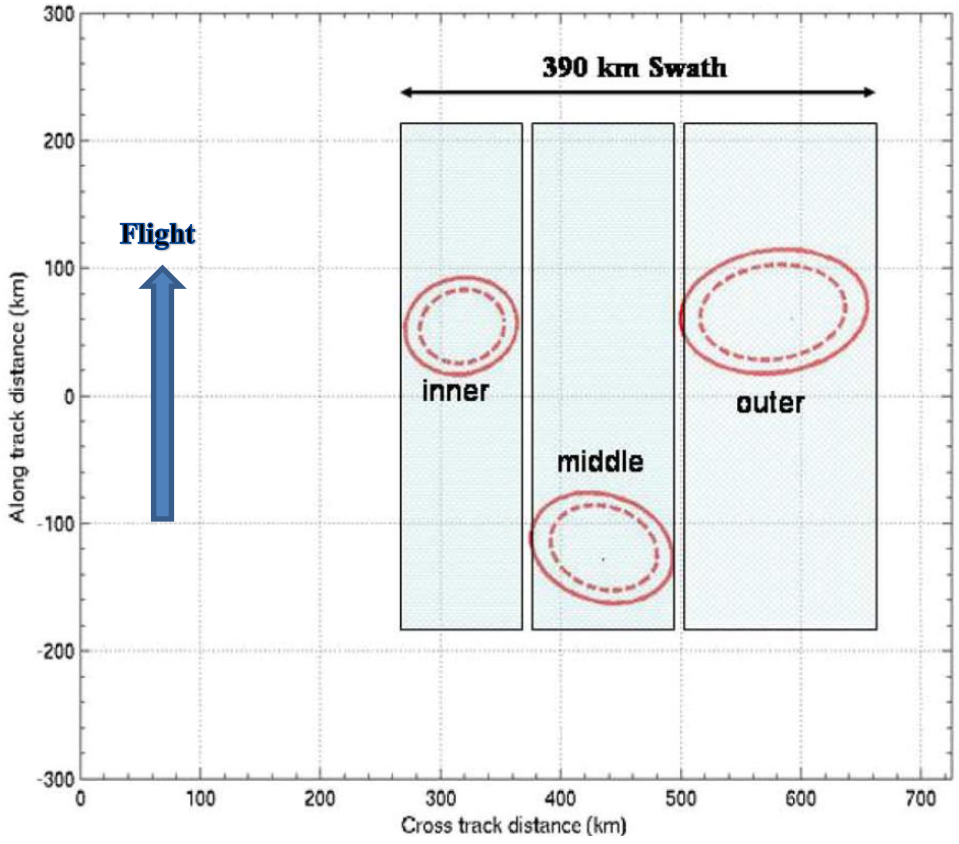

Figure 3 AQ Radiometer and Scatterometer 3db Footprints

2.2 Aquarius Measurements

Aquarius/SAC-D observatory will provide the scientists with measurements pertaining salinity, ocean wind speed, rain, sea ice, sea and land surface temperature, soil moisture, high temperature events (e.g. fires and volcanic eruptions), night time light sources, atmospheric temperature and humidity and

information about space environment. But the primary goal of this mission is measuring sea surface salinity, which is retrieved from brightness temperatures measure by AQ instrument.

The process starts with measuring the surface thermal emission and then using this signal to find the brightness temperature (in kelvin). Later, those brightness temperatures will be used to retrieve salinity, in which the ocean water emission is sensitive to salinity at this frequency (L-band) [4].

When a signal propagates through the atmosphere, a combination of atmospheric and space emissions contribute to attenuate and distort the signal, and those emissions must be taken into account in order to maintain the accuracy needed for salinity measurements. Those emissions include upwelling atmospheric emissions, reflected downwelling atmospheric emissions and space emissions [9].

Atmospheric emissions are initiated by the gas content of the atmosphere, clouds, water vapor, cloud liquid water and wind speed (surface roughness). Some of these emissions propagate upward causing upwelling signal and some of them propagate downward causing the downwelling signal that gets reflected back off the ocean's surface. On the other hand, the space contribution includes cosmic background radiation, galactic, solar and lunar direct and reflected radiation [9].

The propagation path also includes the ionosphere, where the earth's magnetic field causes the polarization of the propagating signal to rotate [10]. And that can be a problematic issue, since emissivity depends on polarization. Figure 4 illustrates the noise signals affecting the original signal (Black).

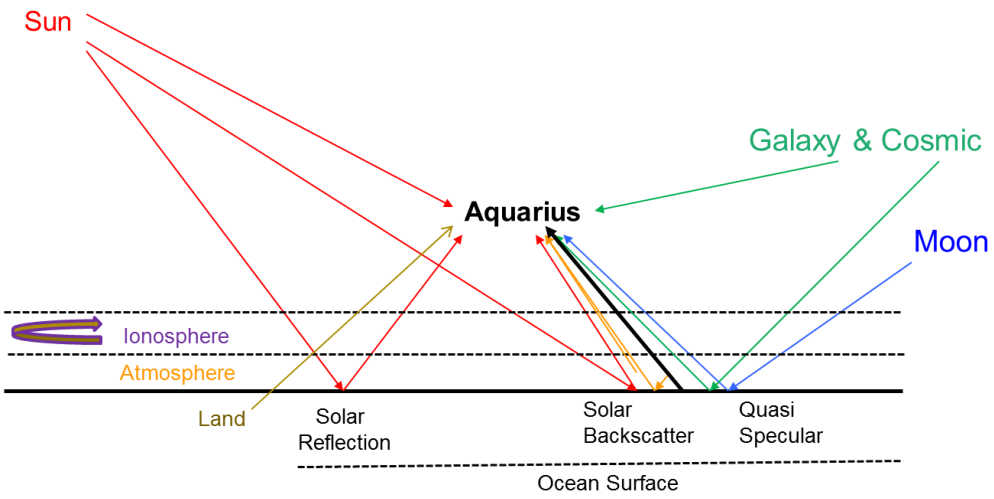

Figure 4 Signals Received by AQ

Errors occurred from the above sources cause attenuations and distortions to be added to the measured signal. AQ measured antenna temperature is filtered to remove those errors separately. A conventional radiative transfer model is used to speculate the attenuations and emissions caused by the atmosphere [11]. The galactic and cosmic backgrounds can be modeled, and those models can be used to characterize their contribution in the measured brightness temperature [12]. Solar radiations are minimized by keeping the Aquarius/SAC-D observatory in a nearly polar, sun-synchronous orbit (equatorial crossings occur at 6:00 am and 6:00 pm) and pointing the beams toward the night side of the orbit. But despite that, solar and lunar radiations manage to reach the radiometer through the side lobes [6]. This kind of occurrences can be accurately predicted and removes from the brightness temperatures. And third stokes parameters (correlation between vertical polarization and horizontal polarization) are measured to retrieve the rotation angle and solve for it [10].

Surface roughness caused by surface wind speed yields and increase in the brightness temperature. And this is the most difficult source of error to correct for, because of the difficulty of characterizing the wave roughened surface.

2.2.1 Aquarius Brightness Temperatures

Surface brightness temperature (T_B) is the microwave signal caused by emissions from the land and sea surfaces, which propagates through the atmosphere. This signal gets attenuated and affected by external sources by the time it gets to the top of the atmosphere; therefore at this point this signal is called the brightness temperature at the top of the atmosphere (T_{toa}).

The signal experiences Faraday rotation of polarization vectors as it travels through the ionosphere (T_{toi}). After that, direct solar and galactic signals are added to it and the new signal is picked up by the horns of the observatory and called apparent aperture temperature (T_A) [9].

Transferred through the feed horns, the orthomode transducer (OMT) and Front-End transmission line until the input of the radiometer, this signal weakens and internal noises are added to it. At this stage the signal is called antenna temperature (T_{ant}) [13]. T_{ant} then is converted to counts as shown in figure 5 that shows AQ block diagram.

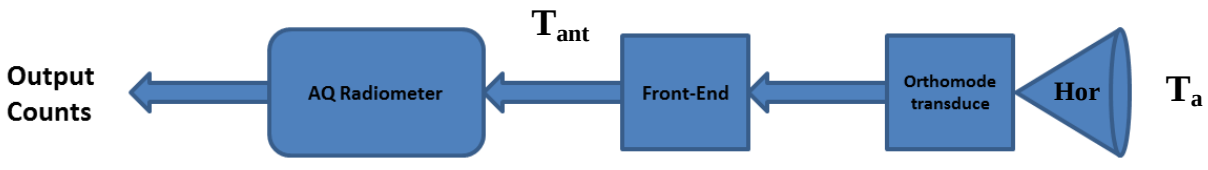

Figure 5 AQ Block Diagram

Each radiometer of AQ is a three states Dicke radiometer (Antenna, Dicke load, Noise diodes) to help calibrating and measuring the radiometer gain and offset [7]. Noise diodes, internal losses and temperatures are adequately calibrated and modeled, and are used to convert radiometer counts to measured antenna temperatures (T_{ant}) and then to apparent temperature (T_A) [13] as shown in figure 6.

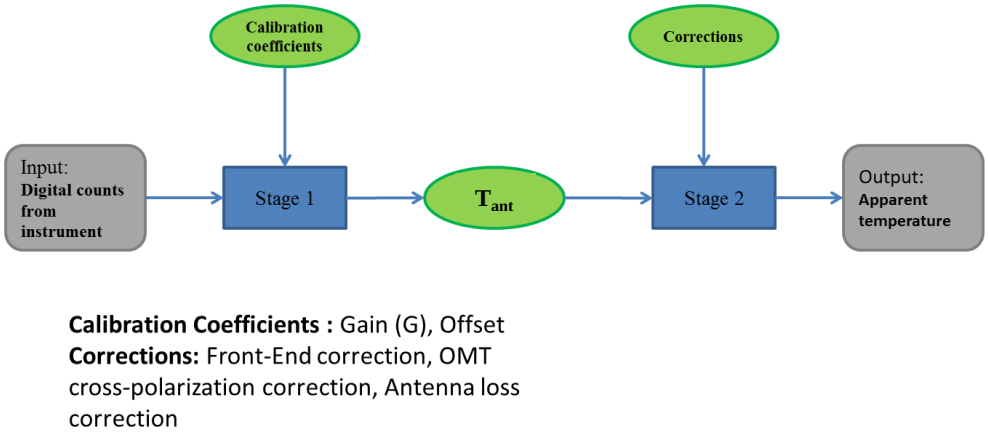

Figure 6 Inverse Model Block Diagram (First Step)

An inverse model is dictated to reconvert T_A back to T_B. Figure 7 illustrates the block diagram of the inverse model.

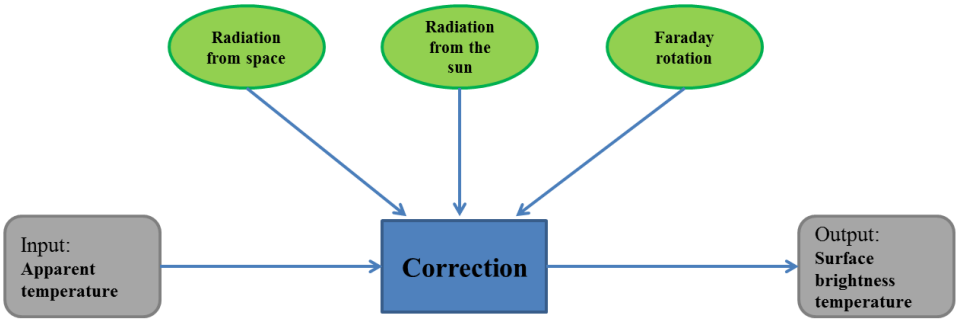

Figure 7 Inverse Model Block Diagram (second step)

Using vertical polarization and horizontal polarization, the first, second and third stokes of the measurement vector $T_{A,mea}$ (apparent temperature vector) are generated. $T_{A,mea}$ is shown in equation (1) [14]:

$$T_{A,mea} = \begin{bmatrix} T_{A1,mea} \\ T_{A2,mea} \\ T_{A3,mea} \end{bmatrix} = \begin{bmatrix} T_{A,mea,V} + T_{A,mea,H} \\ T_{A,mea,V} - T_{A,mea,H} \\ T_{A,mea,+45} - T_{A,mea,-45} \end{bmatrix} \quad (1)$$

$T_{A,mea}$ is divided into two components, T_A measured from earth field of view ($T_{A,earth}$) and T_A measured from space field of view ($T_{A,space}$) [14].

$$T_{A,mea} = T_{A,earth} + T_{A,space} \quad (2)$$

And those two components can be calculated as:

$$T_{A,earth} = \frac{1}{4\pi} \int_{earth} G(b) R(\Phi) T_{B,toa} \frac{\partial \Omega}{\partial A} dA \quad (3)$$

$$T_{A,space} = \frac{1}{4\pi} \int_{earth} G(b) T_{B,space} d\Omega \quad (4)$$

The integration in equation (3) is over the Earth's surface, where dA is the differential surface area. While the integration in equation (4) is over space, where $d\Omega$ is the differential solid angle. **G** is the antenna gain function, in which each element in it, is a function of the look direction **b**. For equation (3), **b** is the unit vector pointing from the antenna to dA. And for equation (4), **b** is a unit vector in the direction determined by $d\Omega$ [9].

The term $R(\Phi)$ is the rotation matrix, and Φ is the rotation angle which is a combination of polarization rotation angle and Faraday rotation angle.

Space brightness temperature consists of cosmic background, galactic, solar and lunar components. These radiations reach the antenna either directly or through Earth by reflection and scattering. And those which are reflected and scattered back from Earth are considered within the Earth's component of the radiation.

$$T_{A,space} = T_{A,sun\_direct} + T_{A,galax\_direct} \quad (6)$$

$$T_{A,earth} = T_{A,earth\_direct} + T_{A,sun\_refl} + T_{A,gal\_refl} + T_{A,sun\_scat} + T_{A,moon\_ref} \quad (7)$$

T_{A,sun_direct}, T_{A,sun_refl} and T_{A,sun_scat} are direct, reflected and scattered solar radiation respectively, T_{A,gal_direct}, T_{A,gal_refl} and T_{A,gal_scat} are direct and reflected galactic radiation respectively and $T_{A,moon\_ref}$ is the reflected radiation of the moon, while $T_{A,earth\_direct}$ is the radiation coming directly from the earth [9].

The external antenna temperature terms (space radiation) are directly computed by performing numerical integrations [9]. Figures 8 and 9 show the direct and reflected solar and galactic temperatures compared with the orbital angle over 4 days period for vertical and horizontal polarizations (late August).

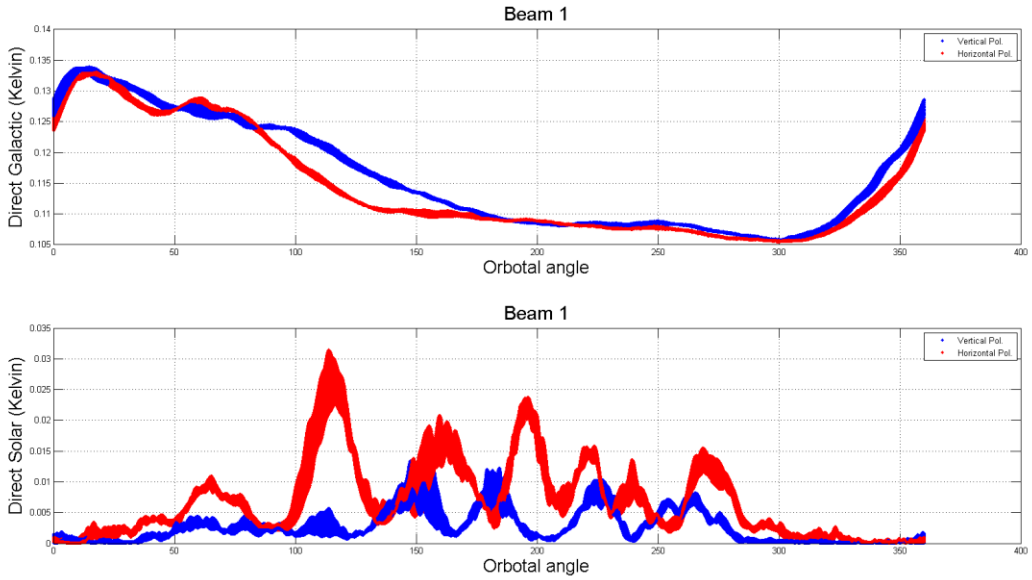

Figure 8 Direct Solar and Galactic Contaminations

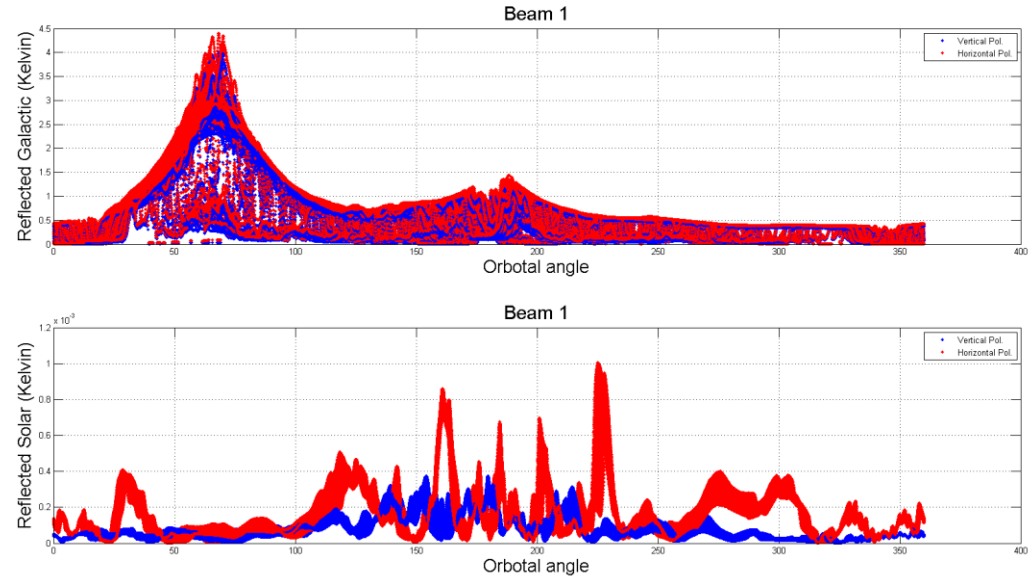

Figure 9 Reflected Solar and Galactic Contaminations

The remaining term of the equation is $T_{A,earth\_direct}$ can be found by subtracting the space radiation contribution from the measure T_a's ($T_{A,mea}$).

$$T_{A,earth\_direct} = T_{A,mea} - T_{A,galax\_direct} - T_{A,gal\_refl} - T_{A,sun\_direct} - T_{A,sun\_refl} - T_{A,sun\_scat} - T_{A,moon\_ref} \quad (8)$$

To estimate T_{toi}, a forward simulation is used [9] as shown in equation (9):

$$T_{toi} = A.T_{A,earth\_dir} \quad (9)$$

Where **A** is antenna pattern correction (APC) matrix (3 by 3).

Faraday rotation perturbs the polarization of the propagating electromagnetic waves and affects the measured brightness temperature by several kelvins. This effect needs to be alleviated to the minimum before those brightness temperatures are used to retrieve salinity [14]. Therefore, next step of retrieving the surface brightness temperature is finding T_{toa} by applying the Faraday rotation correction as shown in equation (10) [9]:

$$T_{toa} = R(\Phi_f)\, T_{toi} \quad (10)$$

Where Φ_f is the Faraday rotation angle that can be found using the third and second stokes as shown below:

$$\Phi_f = \frac{1}{2}\tan^{-1}\left(\frac{T_{toi,3}}{T_{toi,2}}\right) \quad (11)$$

And

$$R(\Phi_f) = \begin{bmatrix} 1 & 0 & 0 \\ 0 & cos2\emptyset & -sin2\emptyset \\ 0 & sin2\emptyset & -cos2\emptyset \end{bmatrix} \quad (12)$$

To abolish the Faraday rotation, equation (11) is substituted in the rotation matrix in equation (12) and then in equation (10), which will treat each of the stokes separately to speculate the first and the second stoke of T_{toa} [16].

The first stoke is not radically affected by the Faraday rotation, hence, the first stoke of T_{toi} and first stoke of T_{toa} are equal. But this is not the situation for the second stoke [16].

$$T_{toa}(1) = T_{toi}(1) \tag{13}$$

$$T_{toa}(2) = \sqrt{T_{toi}^2(2) + T_{toi}^2(3)} \tag{14}$$

Afterward, the conventional polarization (V, H) are calculated [16].

$$T_{toa,V} = \frac{T_{toa}(1)+T_{toa}(2)}{2} \tag{15}$$

$$T_{toa,H} = \frac{T_{toa}(1)-T_{toa}(2)}{2} \tag{16}$$

$T_{toa,V}$ and $T_{toa,H}$ are the vertical and horizontal brightness temperature at the top of the atmosphere respectively.

The signal at the top of the atmosphere is reliable to be used in the Radiative Transfer Model (RTM) to calculate the surface brightness temperature. It comprises upwelling signal, reflected downwelling signal reflected extraterrestrial (cosmic) signal and the surface emission signal [9], as shown in Figure 10.

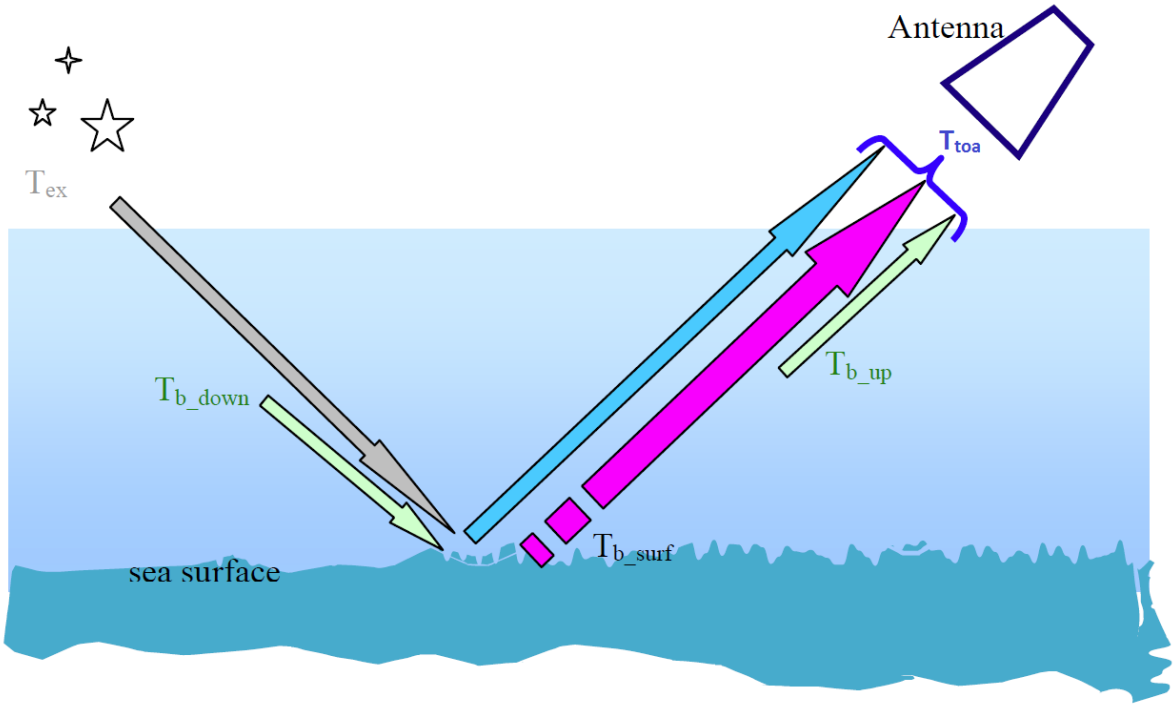

Figure 10 RTM Signals

$$T_{toa} = T_{up} + \tau \times [\varepsilon T_s + (1-\varepsilon)T_{dwn} + (1-\varepsilon)\tau T_{ex}] \quad (17)$$

T_{up} is the upwelling temperature, T_{dwn} is the downwelling signal, T_{ex} is the extraterrestrial back scatter signals (T_{cosmic}), T_s is the physical temperature of the sea surface, ε is the surface emissivity and (τ) is the transmittance of the atmosphere, which is computed by using the NCEP profiles of pressure, temperature, humidity and liquid water.

The T_s are taken from the NCEP daily product (Earth gridded over 0.25 degree boxes) [9], and therefore, the emissivity can be given as:

$$\varepsilon_P = \frac{\frac{T_{toa,P} - T_{up}}{\tau} - (T_{dwn} + \tau T_{ex})}{T_s + (T_{dwn} + \tau T_{ex})} \quad (18)$$

Surface brightness temperature measured by Aquarius can be found as:

$$T_{B,P} = \varepsilon_P \times T_S \quad (19)$$

The amount of ocean emission is different from H pol to V pol (~40% H pol, ~60% V pol) and is highly polarized, and also has incidence angle dependence. Figures 11 through 13 show Ocean's T_{BV} versus T_{BH} at 28.7°, 37.8° and 45.6° respectively in which land and ice contaminations are filtered out.

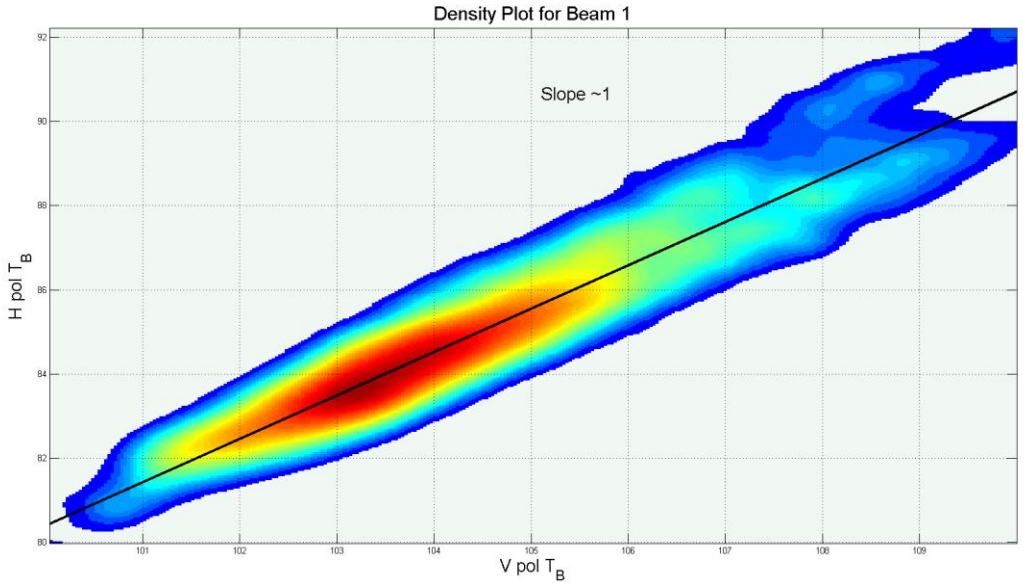

Figure 11 Beam 1 T_B Comparison

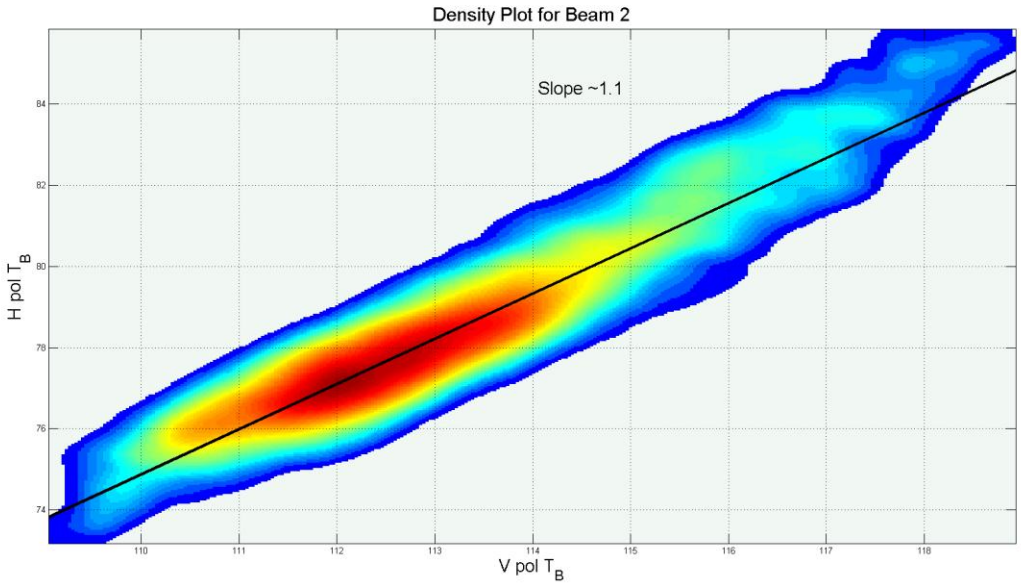

Figure 12 Beam 2 T_B Comparison

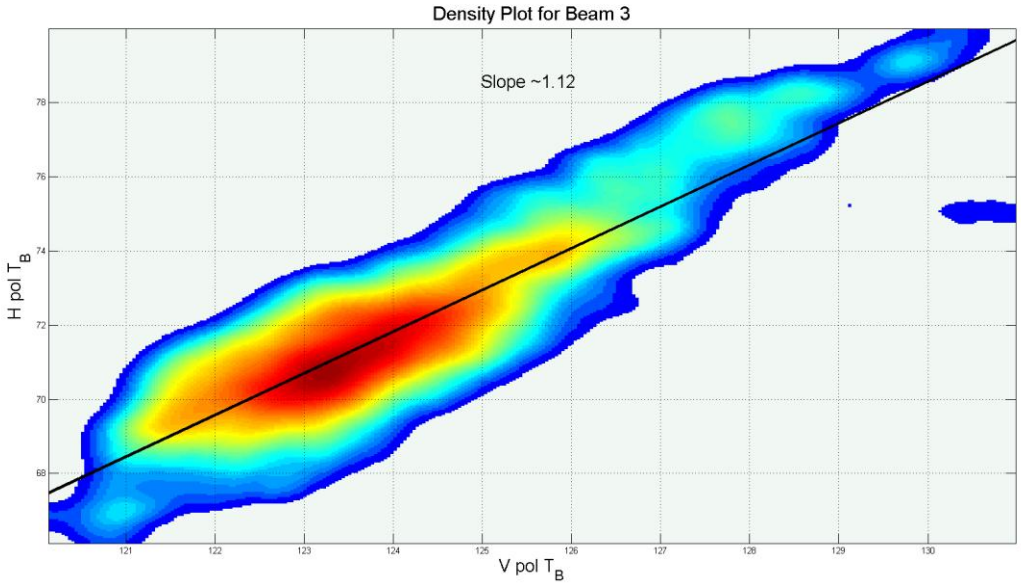

Figure 13 Beam 3 T_B Comparison

2.2.2 Aquarius Salinity Retrievals

The ocean surface emissivity depends on surface temperature T_s, sea surface salinity SSS, Earth incidence angle, polarization and surface roughness (Horizontal polarization is more sensitive to surface roughness than Vertical polarization) which is a function of wind speed and direction [6].

The wind direction effect of the surface emission shall be removed before retrieving the salinity:

$$T`_B = T_B - [p_1(\theta_i)cos(\emptyset_r) + p_2(\theta_i)\cos(2\emptyset)]\, W\, T_s \quad (20)$$

$T`_B$ is the surface brightness temperature with the wind direction effect removed. $\mathbf{p_1}$ and $\mathbf{p_2}$ are coefficient, θ_i is the incidence angle, $\emptyset_r$ is the direction of wins relative to the azimuth angle of the AQ beam look direction and W is the wind speed [9].

Vertical $T`_B$ only is used in the algorithm to retrieve salinity [6] because it is less sensitive to wind speed ton provides more reliable retrievals:

$$SSS = function(\theta_i, WS, T_s) \quad (21)$$

For a certain incidence angle (θ_i) and sea surface temperature (SST), the relation between the brightness temperature and the SSS is almost linear. Figures 14 through 19 illustrate the relation between T_{BV} and T_{BV} versus salinity at 28.7°, 37.8° and 45.6° respectively and at 299 K SST over a 4 days period.

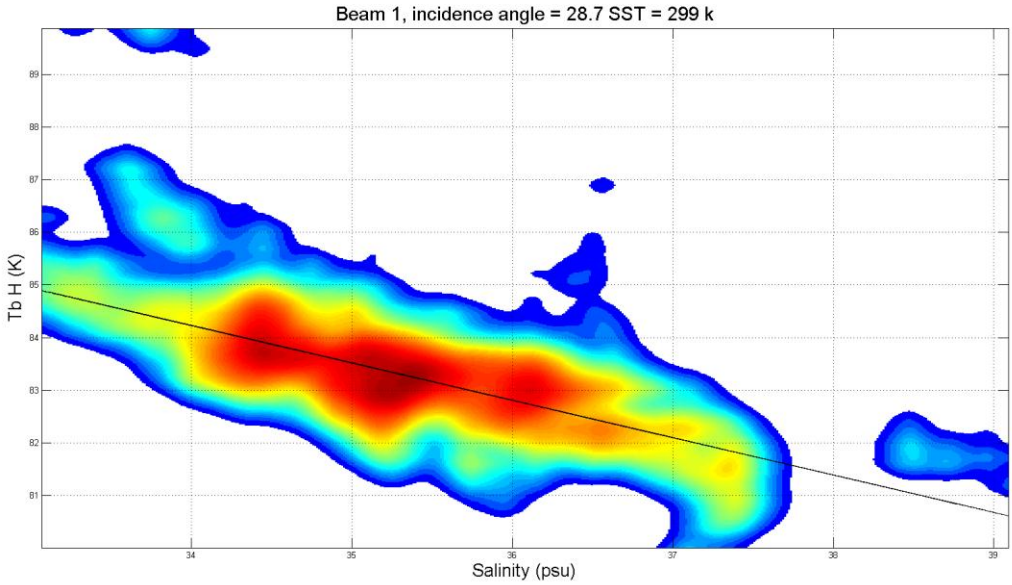

Figure 14 Horizontal T_B versus Salinity (Beam 1)

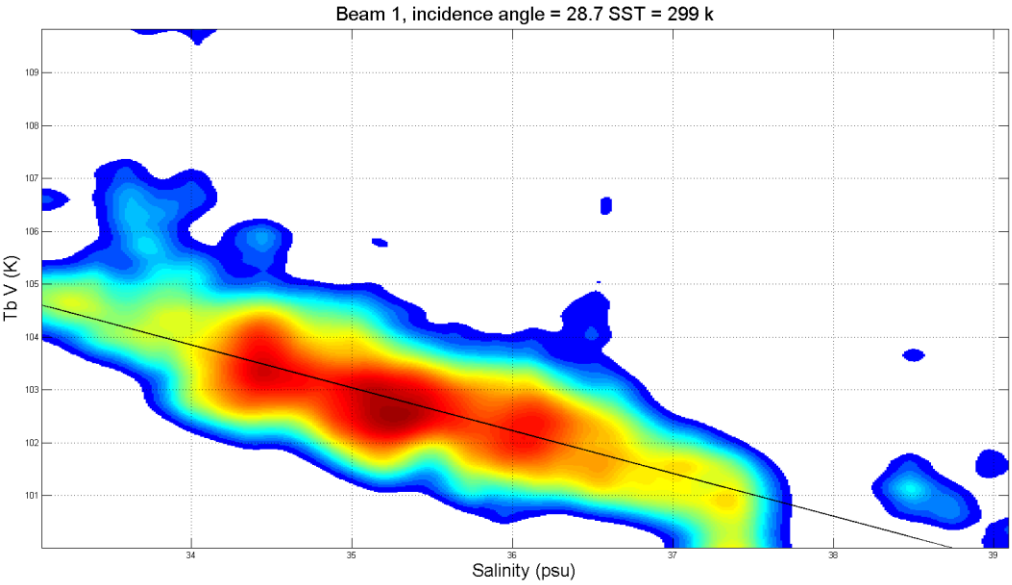

Figure 15 Vertical T_B versus Salinity (Beam1)

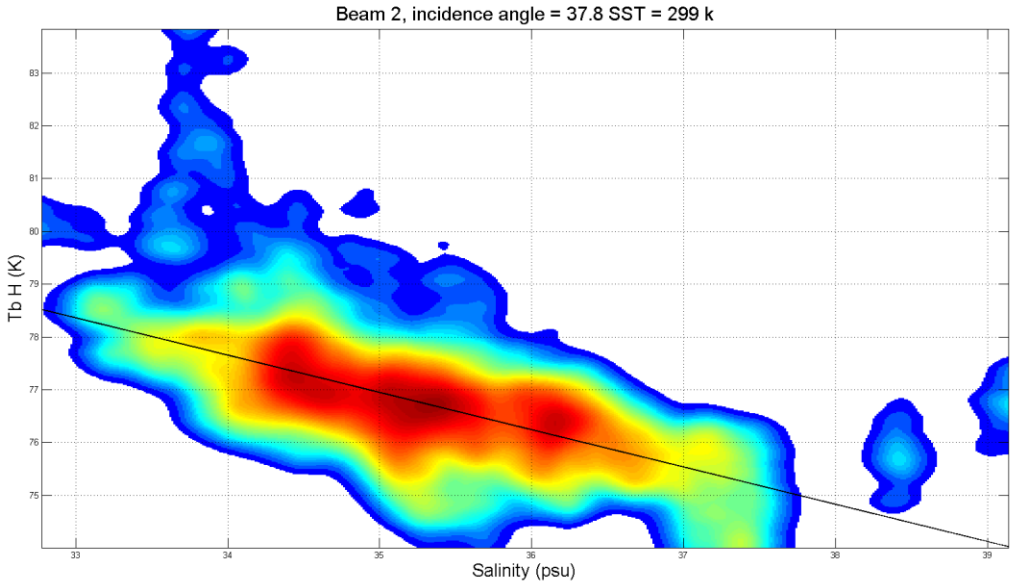

Figure 16 Horizontal T_B versus Salinity (Beam 2)

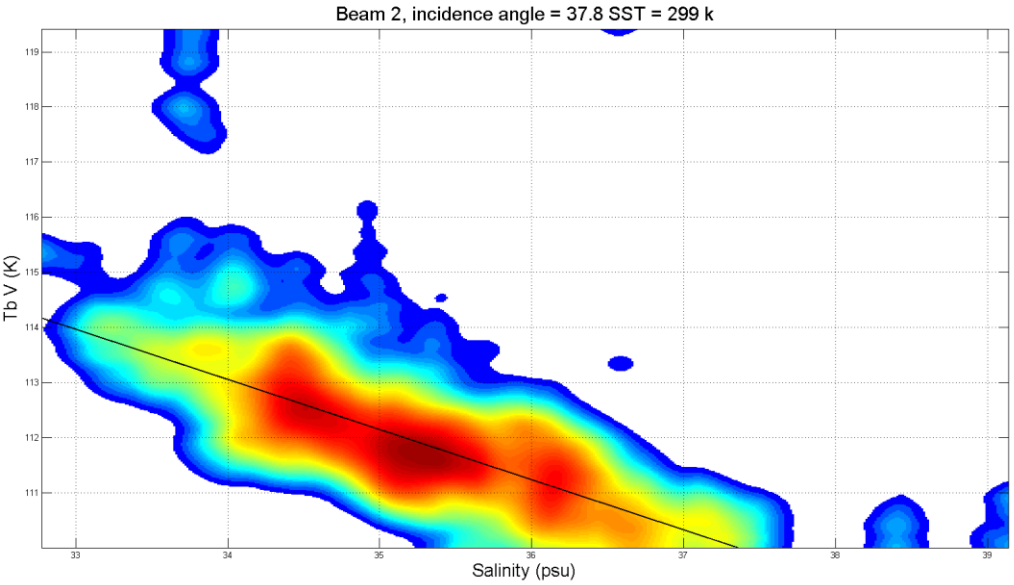

Figure 17 Vertical T_B versus Salinity (Beam 2)

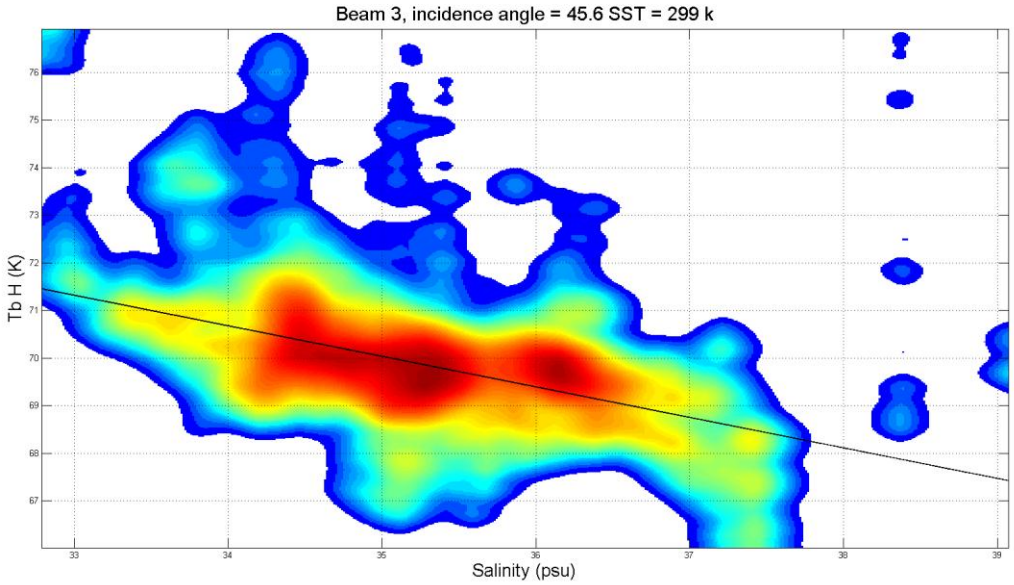

Figure 18 Horizontal T_B versus Salinity (Beam 3)

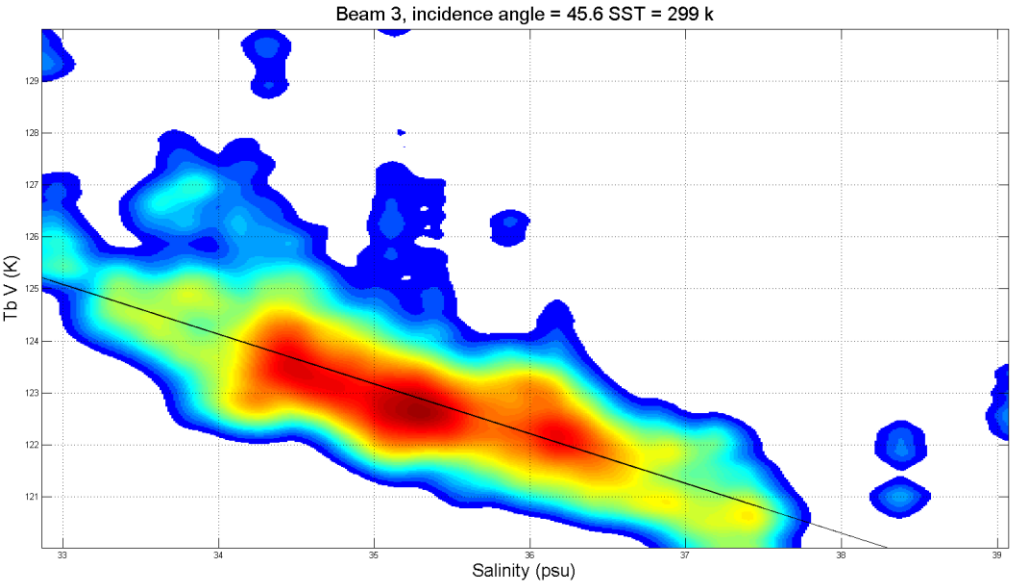

Figure 19 Vertical T_B versus Salinity (Beam 3)

CHAPTER THREE: AQ DATA ANALYSIS

3.1 Salinity Algorithm

After correcting the measured brightness temperature for the wind direction effect, Ocean surface emissions depend on T_S, SSS, and incidence angle and ocean roughness (wind speed only).

$$T_B = SST \times \varepsilon(T_S, SSS, WS, \theta_i) \quad (21)$$

In early stages, an emissivity model is used to find the value of the salinity at specific geophysical parameters (WS, SST), incidence angle and surface brightness temperature [16].

This algorithm can be presented as the following equation:

$$SSS = a_o(\theta_i, ws, SST) + a_1(\theta_i, ws, SST)\, T`_B \quad (22)$$

The ***a*** coefficients are functions of incidence angle and sea surface temperature are in tabular form and they are functions of wind speed and sea surface temperature [6]. The model is only applied to the vertical polarization only (physical characteristics of vertical polarizations make it more reliable in measuring salinity [17])

The algorithm will be trained by empirically estimating the ***a*** coefficients that will mitigate the error between the modeled salinity and the true salinity measured using the *in situ buoys* [17]. The algorithm validation requires to compute $T`_B$ over a full range of SSS, SST, and WS for a certain incidence angle.

The salinity retrieval is very sensitive to WS. Blowing winds add an excess brightness temperature to the measured T_B, which in turn adds an excess salinity to the retrieved. Brightness temperature changes about 0.2K-0.3K for every 1m/s change in wind speed and that will introduce the salinity retrieval error of 1 psu for warm water (25^{o}C) and more than 2 psu for cold water(5^{o}C) [18], and therefore, a precise correction technique should be implemented to achieve an accuracy of 0.2 psu. Figures 20 to 23 show the relation

between the WS and T_B for both vertical and horizontal polarizations respectively at 28.7°, 38.7° and 45.6° incidence angles over SSS= 34 psu and SST= 300 K.

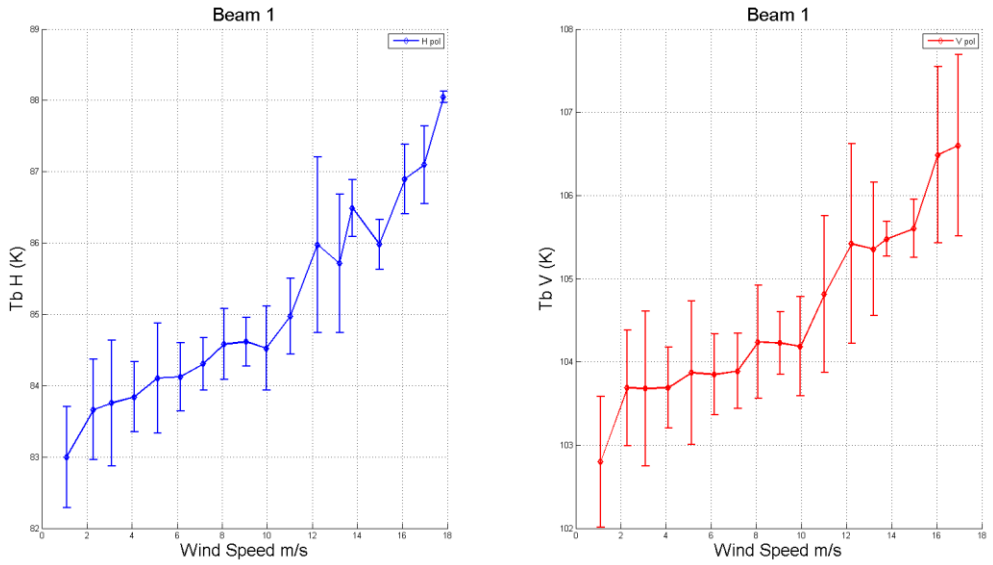

Figure 20 WS versus T_B at 28.7° for SST=300K and SSS=34psu

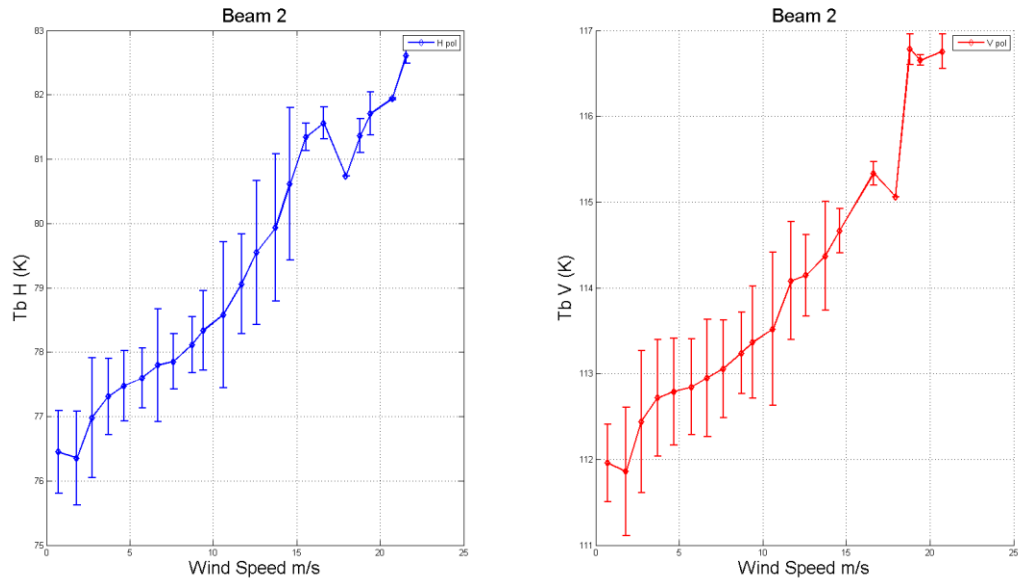

Figure 21 WS versus T_B at 37.8° for SST=300K and SSS=34psu

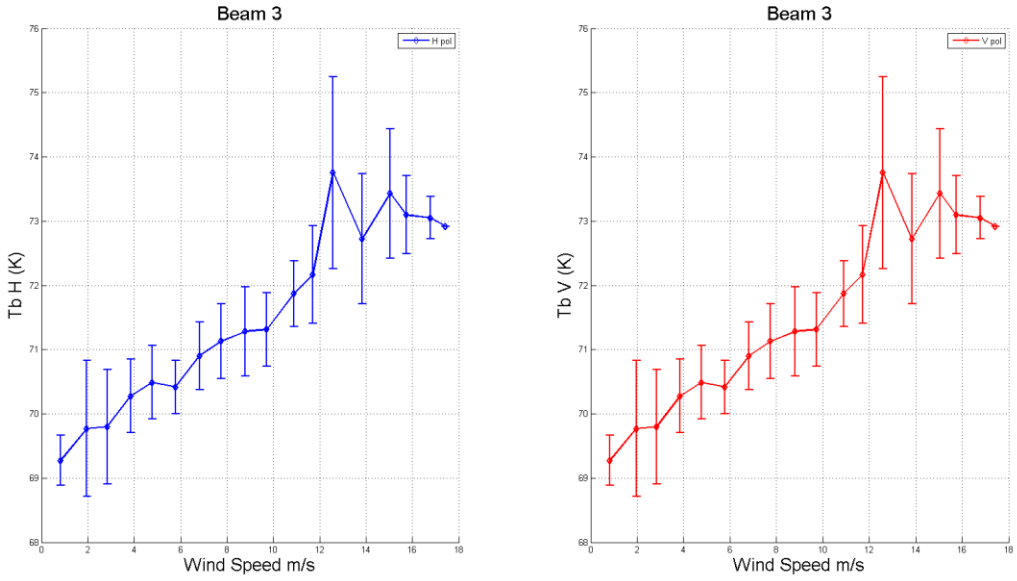

Figure 22WS versus T_B at 45.6° for SST=300K and SSS=34psu

3.2 Ocean Roughness Correction

When the wind blows over the ocean's surface, waves from the surface roughness increase, yielding drastic changes in ocean surface reflectivity and therefore, the surface emission is increased [20] as shown in equation (23) (CFRSL emissivity model):

$$\varepsilon(SST, SSS, WS, \theta_i) = \varepsilon_{smooth}(SST, SSS, \theta_i) + \Delta\varepsilon_{excess}(WS) \quad (23)$$

And therefore the modeled brightness temperature which is used to estimate the excess brightness temperature can be found as [18]:

$$T_B(SST, SSS, WS, \theta_i) = T_{B,smooth}(SST, SSS, \theta_i) + \Delta T_{B,excess}(WS) \quad (24)$$

The brightness temperature at zero wind speed is called the smooth brightness temperature ($T_{B,smooth}$), and can be determined by calculating the water emissivity using the Klein and Swift dielectric model [18]. The excess brightness temperature is the error induced by the wind, and for a certain SST and SSS, it's a function of wind speed only.

The main approach is to use the CFRSL model to calculate an excess brightness temperature, and then subtract it from the measured surface brightness temperatures to find the smooth brightness temperature that is used to retrieve salinity as shown on figure 23.

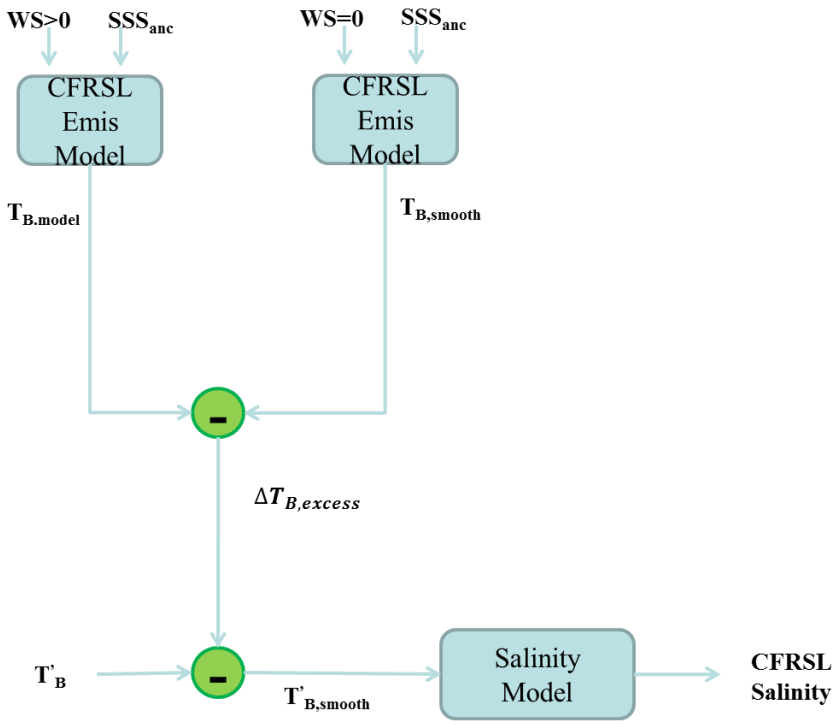

Figure 23 Correction Algorithm

SSS_{anc} is the ancillary salinity derived from the HYCOM model (described in section 4.1), it is salinity maps generated by averaging the In-Situ measurements every 6 hours every day that give a close estimation of the actual salinity values of the ocean.

To model the excess brightness temperature, CFRSL emissivity model has been developed to relate the geophysical parameters (SSS, SST, WS) to surface emissivity. And this model comprises two parts: smooth surface emission and rough ocean surface emission [19] as shown in equation (24).

Smooth ocean surface emission can be determined by setting the WS parameter to zero which will converge the excess term of the equation to zero, and therefore the excess surface emission due to wind speed can be estimated as:

$$\Delta T_{B,excess} = T_{B,model} - T_{B,smooth} \quad (25)$$

Figure 23 to 28 show the relation between the wind speed and the excess brightness temperature for the vertical polarization at 28.7°, 37.8° and 45.6° respectively.

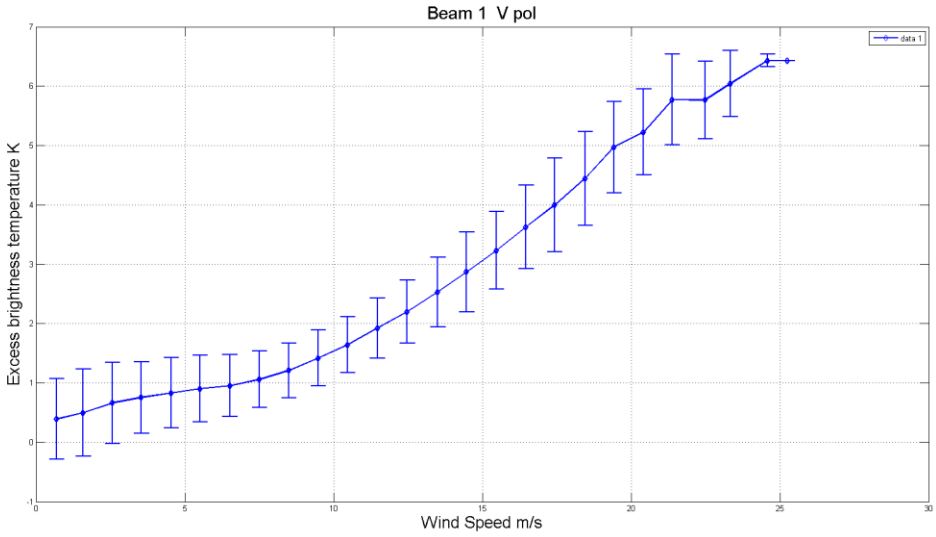

Figure 24 WS versus Excess TbV at 27.8°

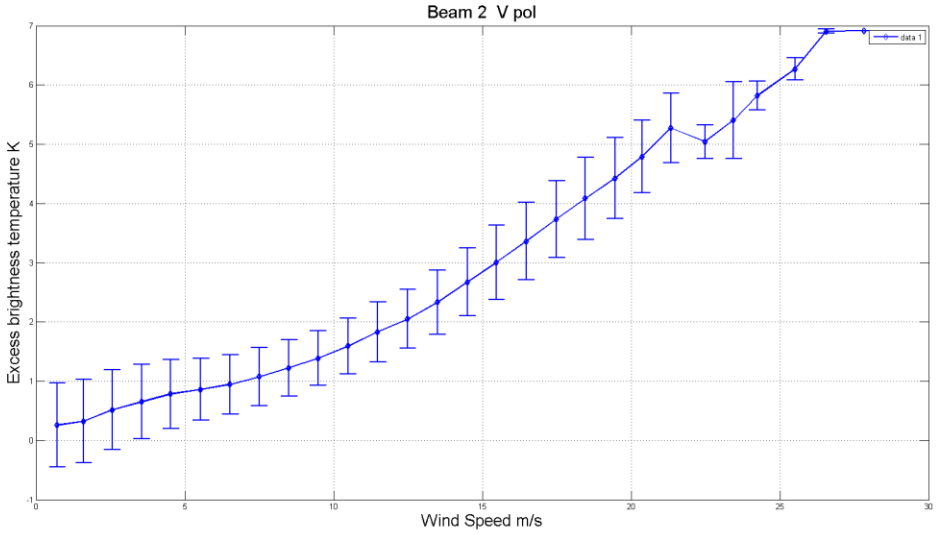

Figure 25 WS versus Excess TbV at 37.8°

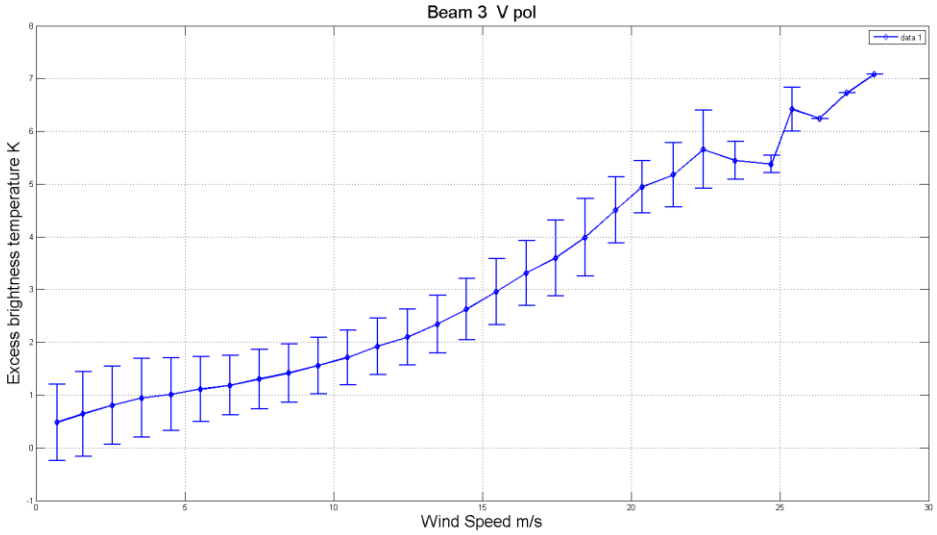

Figure 26 WS versus Excess TbV at 45.6°

This dependent on wind speed can be modeled as:

$$\Delta Tb_{rough} = \left.\frac{\partial Tb_{meas}}{\partial WS}\right|_{SST=const} * \Delta WS \qquad (26)$$

ΔTb_{rough} is the excess brightness temperature due to wind speed, $\frac{\partial Tb_{meas}}{\partial WS}$ is the rate of change in brightness temperature due to wind speed and ΔWS is the wind speed range (0 – 20 m/s). Table 3 shows the rate of change for each of the polarizations for the three incidence angle.

Table 3 T_B Rate of Change Due to Wind Speed

Polarization	Incidence angle	$\frac{\partial Tb_{meas}}{\partial WS}$
Vertical	28.7°	0.27091
Vertical	37.8°	0.25911
Vertical	45.6°	0.24605

Since the brightness temperature comprises two parts the measured salinity will have two parts as well, salinity due to smooth ocean surface and salinity due to rough Ocean surface [18]:

$$SSS = SSS\_smooth + \Delta SSS \quad (27)$$

Equation (25) provides a very accurate estimate of the excess brightness temperature using the modeled brightness temperatures, that is used to calculate the smooth surface brightness temperature from the Aquarius measured brightness temperatures

$$T'_{B,smooth} = T'_{B,meas} - \Delta T_{B,excess} \quad (28)$$

After correcting for the wind speed effect, smooth salinity retrievals due to smooth brightness temperature can be found using equation (22):

$$SSS_{smooth} = a_0 + a_1 T`_{B,smooth} \quad (29)$$

The rate of change is salinity due to changes in brightness temperature can be presented as:

$$\Delta SSS = \left.\frac{\partial SSS}{\partial Tb}\right|_{SST=const} * \Delta Tb \tag{30}$$

Table 4 shows the rate of change in salinity due to the change in excess brightness temperature:

Table 4 SSS Rate of Change Due to Excess T_B

Polarization	Incidence angle	$\frac{\partial Tb_{meas}}{\partial WS}$
Vertical	28.7°	0.32795
Vertical	37.8°	0.30529
Vertical	45.6°	0.27688

Since excess brightness temperature is directly related to wind speed changes, the excess salinity can be presented as:

$$\Delta SSS = \frac{\partial SSS}{\partial Tb} \times \frac{\partial Tb}{\partial WS} \times \Delta WS \tag{31}$$

Figures 29 to 34 show the relation between the wind speed and the excess salinity for vertical polarization at 28.7°, 37.8° and 45.6° respectively.

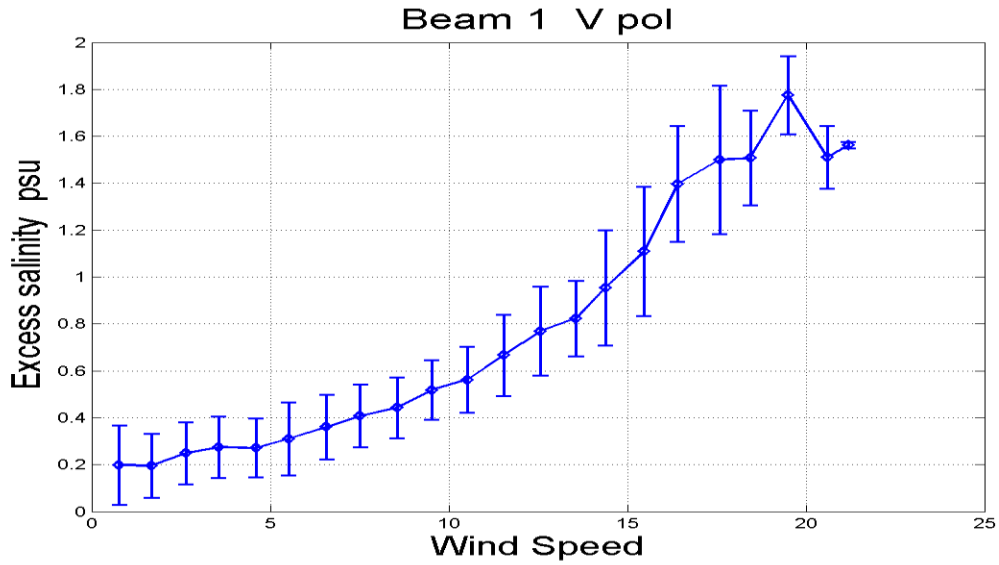

Figure 27 Excess Salinity Due to WS for V pol Beam 1

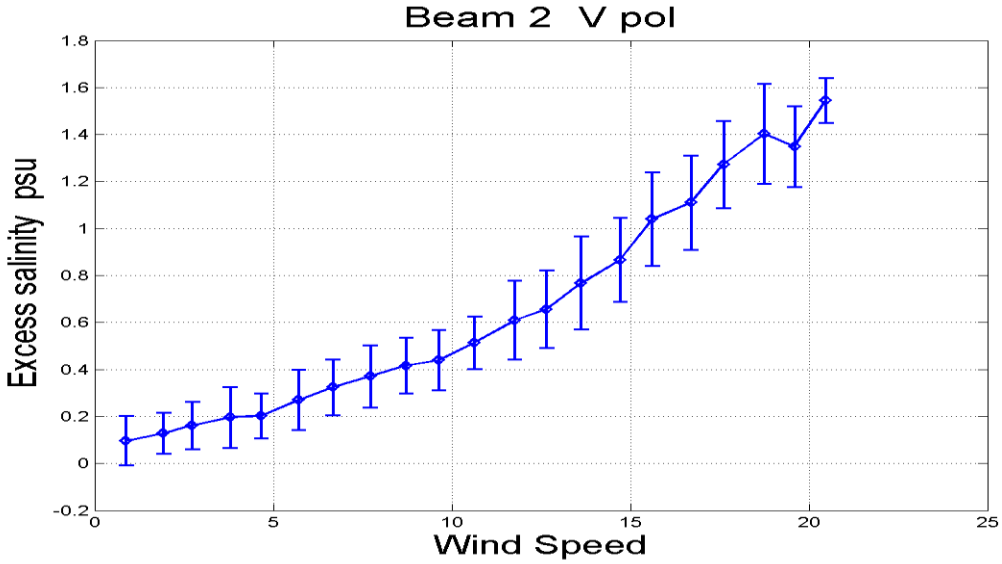

Figure 28 Excess Salinity Due to WS for V pol Beam 2

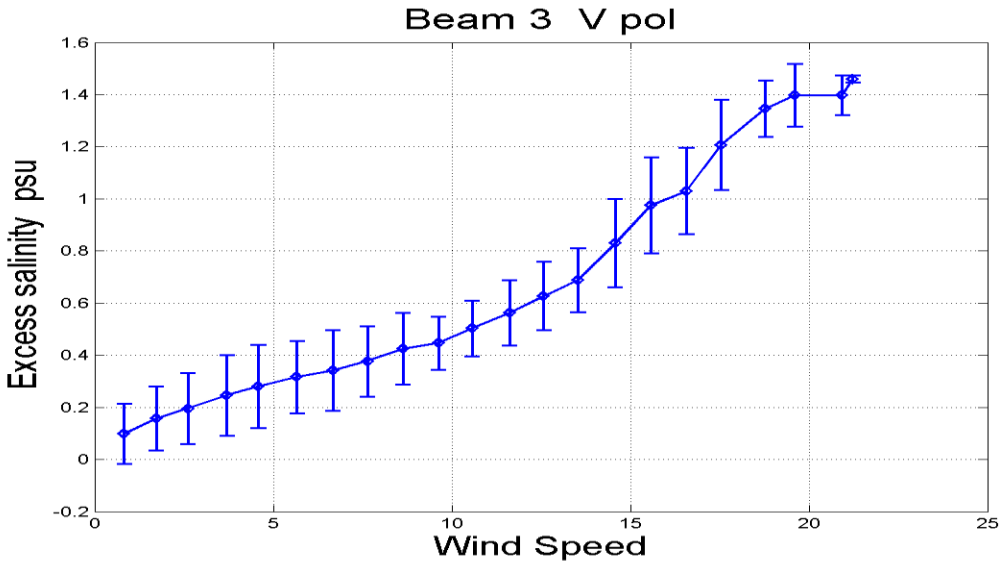

Figure 29 Excess Salinity Due to WS for V pol Beam 3

The corrected salinity (SSS_{smooth}) equals:

$$SSS_{smooth} = SSS_{meas} - \Delta SSS \quad (32)$$

Figure 35 shows a global 7-days salinity map, generated using the smooth surface salinity retrieved from the smooth surface brightness temperatures measured by Aquariu.

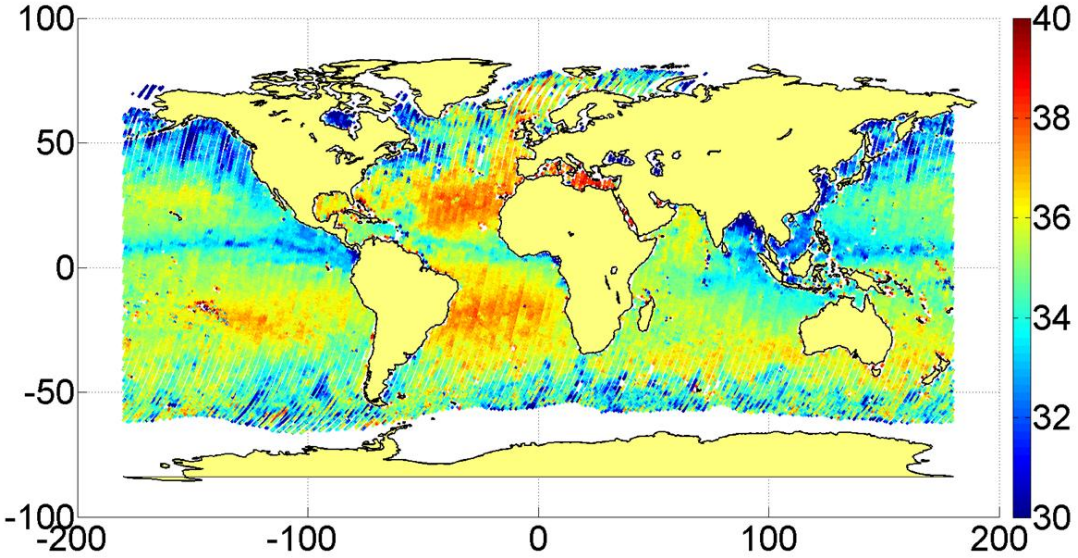

Figure 30 Global Salinity Map for 7-Day Period

CHAPTER FOUR: RESULTS AND VALIDATION

4.1 The Hybrid Coordinate Ocean Mode (HYCOM)

"HYCOM was developed by the HYCOM Consortium, which is part of the U.S Global Ocean Data Assimilation Experiment (GODAE)" [21]. Its main goal it to provide global maps of sea surface salinity averaged every 6 hours.

The main approach is to collect data from all the world's oceans and seas, measured by the In Situ Buoy (shown in figure 35) over long time period and long distances apart, to create 6 hours maps of ocean salinity (shown in figure 36).

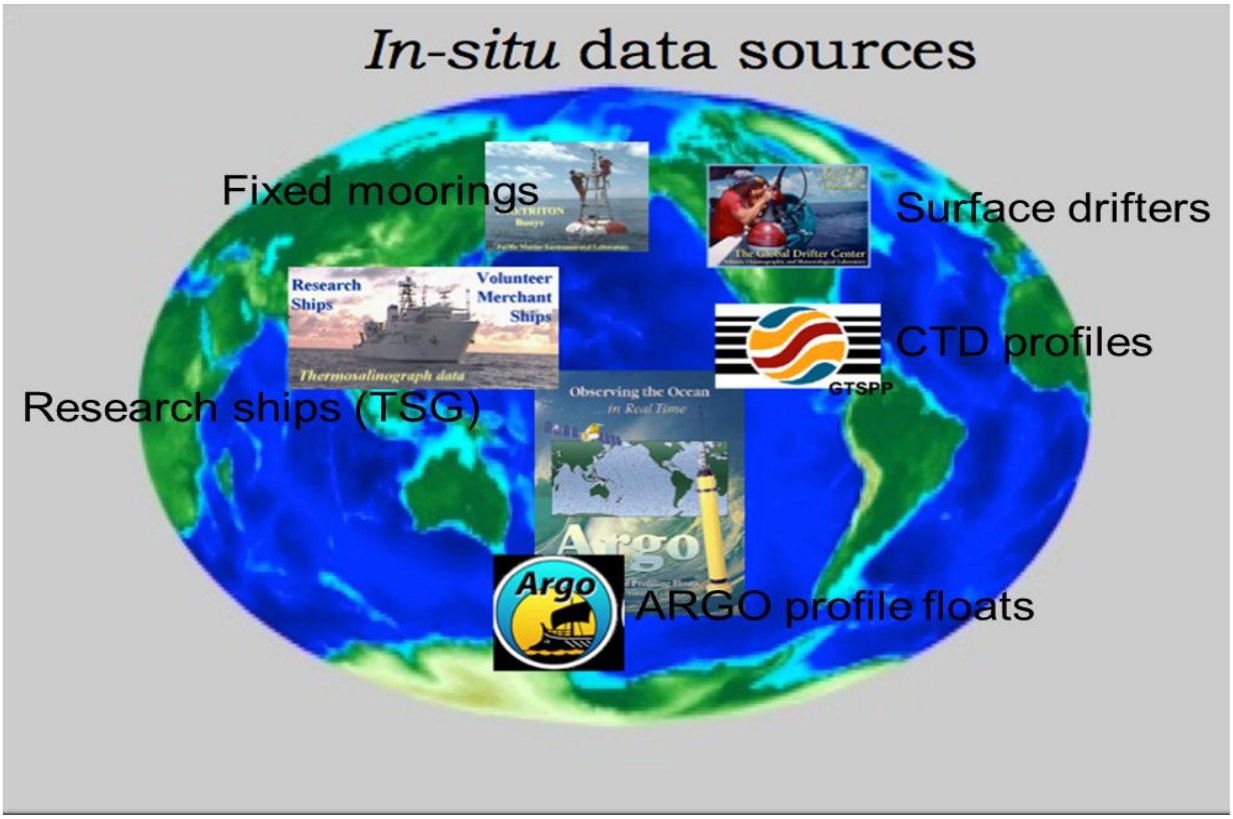

Figure 31 In-Situ Data Sources

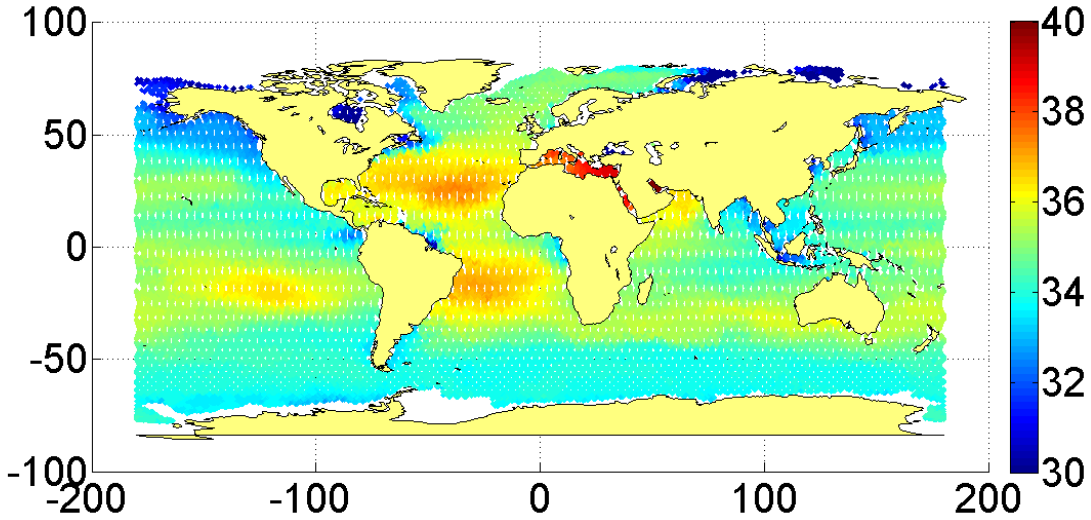

Figure 32 Global Salinity Map Using HYCOM

The HYCOM salinity is a smoothened salinity that shows an average of the global salinity and unable to detect the region with high wind speeds and high rain precipitations, but yet, it is the one of the most reliable model for salinity since it collects data of physical salinity from various parts of the ocean using different means, as shown in figure 37.

HYCOM salinity was collocated spatially and in time with AQ orbits to provide a preliminary estimate of the performance of the forward model and the salinity model.

4.2 Validation

Aquarius provides a global salinity measurement with a resolution of 150 km, which measurements are continuous in time. A 7 days cycle is required for Aquarius to provide a global image of sea surface salinity that is comparable with the HYCOM model salinity.

The HYCOM was collocated with the AQ longitudes and latitudes given each orbit's time. The difference between the HYCOM and AQ salinity was then found as shown in equation 32:

$$\Delta SSS_{validat} = SSS_{HYCOM} - SSS_{smooth} \quad (32)$$

Histograms show the distribution function of the differences shown in figure 37, per beam.

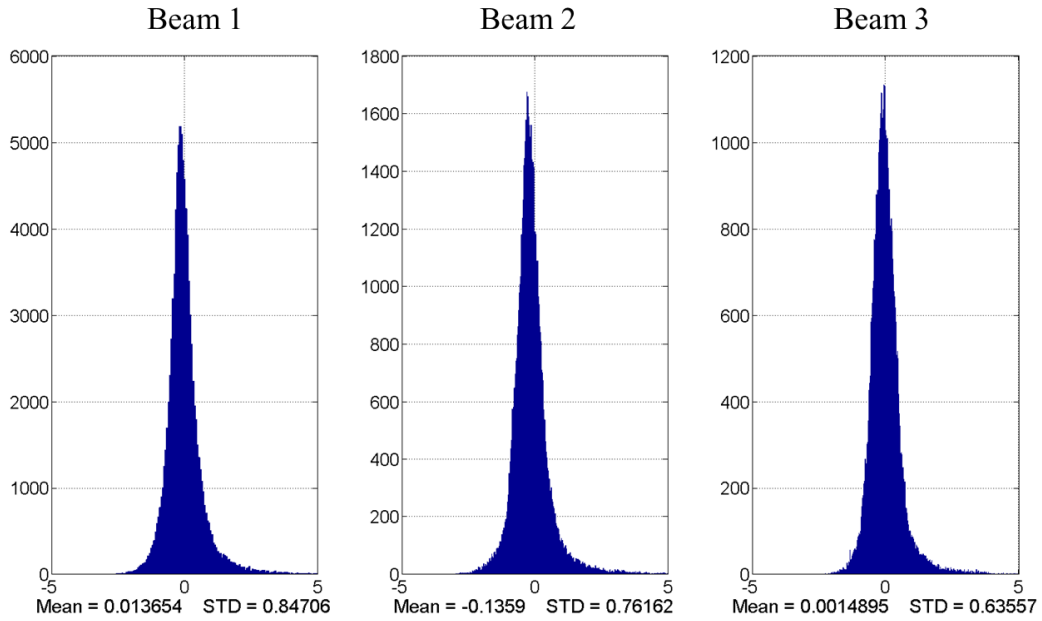

Figure 33 Salinity difference Per Beam

The differences are following a nearly perfect Gaussian distribution, which shows that the mean number of salinity values are less than $|2|psu$. Variations with the mean values between the beams are due to different incidence angles effect, and also the geometry of the beams intersecting the surface of the earth at three locations within the 150 Km swath.

Wind speed effect is eliminated from the corrected salinity retrievals, figure 38 shows the relation between wind speed and $\Delta SSS_{validat}$.

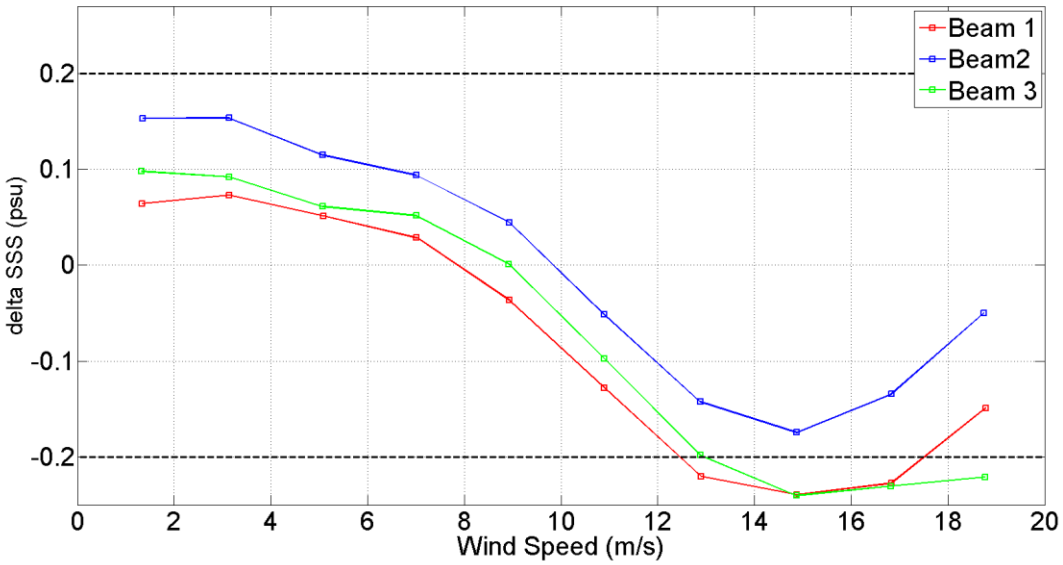

Figure 34 Salinity Differences Relation With Wind Speed

The figure is a binned average representation of the relationship between $\Delta SSS_{validat}$ and the wind speed, averaged every 2 m/s for each beam separately. Every 2 m/s, the average $\Delta SSS_{validat}$ and the average WS is calculated and represented by a dot. And as illustrated, the majority of the points are within the accuracy region of 0.2 psu error budget.

Some points are showing discrepancy, and that is related to the fact that comparing an instrument measurements in real time with a model of averaged data, taken at various periods of time and difference locations cannot be credible where rain exists, near land borders and also over areas where physical measurements were not taken by the In-Situ.

CHAPTER FIVE: CONCLUSION AND FUTURE WORK

5.1 Conclusion

Sea surface salinity is a major factor for tracing the global water cycle. Geophysicists can use it to understand the processes of natural precipitation, evaporation, freezing and melting of ocean water and this was the motive for NASA to start the Aquarius mission with CONAE, which goal, is to provide global salinity measurements and weekly salinity maps of the entire ocean.

The endeavor of the research is to correct the retrieved salinity for the wind speed effect, where the ocean waves agitated by blowing winds, will add an excess brightness temperature to the smooth ocean brightness temperature which will change the salinity measurements by few degrees of psu. An algorithm to correct for the geophysical parameters effect was proposed, calibrated and validated.

A Radiative Transfer Model is applied and simulated to covert the measured output counts to surface brightness temperature. At first the count are converted to antenna temperatures T_{ANT} at the input of the radiometers, using pre-launch calibrated coefficients, and then a correction model is used to find the apparent temperatures T_A.

An inverse model simulates the direct space T_B, reflected space T_B and the atmospheric T_B. the output of this model is the surface brightness temperature (including roughness).

The CFRSL emissivity model, corrects for the wind speed excess T_B vertical polarization (only Vpol is used to retrieve salinity) using equation (25), to calculate ΔT_{excess} that is then subtracted from the AQ measured brightness temperature $T'_{B,meas}$ to find $T'_{B,smooth}$ that is used to find the smooth salinity.

To validate the algorithm, the output salinity is compared to the HYCOM salinity (global model). The comparison is done by finding the difference between the HYCOM salinity and the retrieved salinity (equation 32).

The comparisons show that the mean number of points falls within the desired range of accuracy. Points closer to the land or over rainy regions may show discrepancies higher or lower than the $\pm 2\ psu$, and that is due to the fact of comparing a well calibrated instrument instant measurements to a model that averages various points over the ocean

5.2 Future Work

The Aquarius instrument was launched to space in June 10th, 2011, and still in the test and validation process. Any further changes on the calibration coefficients will require re-tuning of the CFRSL emissivity model to keep matching the AQ instrument. The excess brightness temperatures will be found again to generate the smooth salinity maps to compare with the HYCOM. Furthermore, a better validation and comparisons will need to be implemented using the raw buoy measurement data, which represent the physical measurement of salinity. That will require more work on collocating the AQ boresight location with very little and scattered amount of random points over the oceans. But yet, this will give a better indicating of the validity of the salinity measurements being retrieved by the AQ instrument.

One more important issue is the effect of other geophysical parameters on the AQ measurements, mainly rain. Rain rated derived from the MWR, will be used as rain flags to validate the data set by removing rainy pixels from the analysis, and that will ameliorate the comparisons with the buoy data. The MWR beams are smaller in size, and that will provide a 40 Km resolution as shown in table 2 (an average of 2-3 beam of MWR will be comprised within one AQ beam), and that will require applying a weighted averaging of the MWR rain rate data within each beam of AQ.

LIST OF REFERENCES

[1] G. Lagerloef, F. R. Colomb, D. Le Vine, F Wentz, S. Yueh, C. Ruf, J. Lilly, Y. Chao, A.deCharon, and C. Swift, "The Aquarius/SAC-D mission –Designed to meet the salinity remote sensing challenge," Oceanog. Mag., Mar. 2008.

[2] A. Buis, P. Lynch, G. Cook-Anderson, Ro. Sullivant, "Aquarius/SAC-D: Studying Earth's salty seas from space", Jun. 2011.

[3] D. M. Le Vine, G. S. E. Lagerloef, F. Pellerano, F. R. Colomb, "The Aquarius/SAC-D mission and status of the Aquarius instrument", 2008.

[4] G. Lagerloef, Science Overview, Section 04b, Aquarius/SAC-D Mission CDR package, July 2008.

[5] F. A. Pellerano, J. Piepmeier, M. Triesky, K. Horgan, J. Forgione, J. Caldwell, W. J. Wilson, S. Yueh, M. Spencer, D. McWatters, A. freedman, "The Aquarius ocean salinity mission high stability L-band radiometer", 2006.

[6] D. M. Le Vine, G. S. E. Lagerloef, S. E. Torrusio, "Aquarius and remote sensing of sea surface salinity from space", May 2010.

[7] D. M. Le Vine, G. S. E. Lagerloef, F. Raúrl Colomb, S. H. Yueh, F. A. Pellerano, "Aquarius: An instrument to monitor surface salinity from space", July 2007.

[8] A. Freedman, D. McWatters, M. Spencer, "The Aquarius scatterometer", 2006.

[9] F. J. Wentz, D. M. Le Vine, "Algorithm Theoretical Basis Document: Aquarius salinity retrieval algorithm: final pre-launch version", January 2011.

[10] S. H. Yueh, "Estimates of Faraday rotation with passive microwave polarimetry for microwave remote sensing of Earth surface, 2000.

[11] H.-J. C. Blume, B. M. Kendall, "Passive microwave measurements of temperature and salinity in costal zones", 1982.

[12] D. M. Le Vine, S. Abraham, "Galactic noise and passive microwave remote sensing of sea surface salinity from space", July 2005.

[13] J. Piepmeier, L. Hong, "Aquarius radiometer pre-launch calibration", presented in Algorithm Workshop, Santa Rosa CA USA, March 2010.

[14] S.-B. Kim, F. Wentz, "Brightness temperature retrieval with scale-model antenna pattern of the aquarius L-band radiometer", 2008.

[15] F. J. Wentz, T. Meissner, "Algorithm Theoritical Basis Document: AMSER Ocean algorithm", November 2000.

[16] F. J. Wentz, "Aquarius Salinity Algorithm and Simulation", Presented at Aquarius/SAC-D Science Workshop, Seattle, WA, USA, July 2011

[17] J. Gunn, "Aquarius Validation Data System", Presented at 6th science meeting, Seattle, WA, USA, July 2011

[18] S. H. Yueh, J. Chaubell, "Sea surface salinity and wind retrieval using combined passive and active L-band microwave observations", July 2011

[19] F. Wentz, T. Meissner, "AMSR ocean algorithm", Remote Sensing System, November 2000

[20] S. F. El-Nimri, "Development of an improved microwave ocean surface emissivity radiative transfer model", Doctoral Dissertation, April 2010

[21] Carrie L. Leach, Thomas C. Oppe, William A. Ward, Jr., Roy L. Campell, Jr. "CWO-Based HPCMP Systems Assessment Using HYCOM and WRF", IEE Computer Society, 2005